The Global Climate Response to Lowering Surface Orography of Antarctica and the Importance of Atmosphere–Ocean Coupling

HANSI K. A. SINGH, CECILIA M. BITZ, AND DARGAN M. W. FRIERSON

Department of Atmospheric Sciences, University of Washington, Seattle, Washington

(Manuscript received 25 June 2015, in final form 21 February 2016)

ABSTRACT

A global climate model is used to study the effect of flattening the orography of the Antarctic Ice Sheet on climate. A general result is that the Antarctic continent and the atmosphere aloft warm, while there is modest cooling globally. The large local warming over Antarctica leads to increased outgoing longwave radiation, which drives anomalous southward energy transport toward the continent and cooling elsewhere. Atmosphere and ocean both anomalously transport energy southward in the Southern Hemisphere. Near Antarctica, poleward energy and momentum transport by baroclinic eddies strengthens. Anomalous southward cross-equatorial energy transport is associated with a northward shift in the intertropical convergence zone. In the ocean, anomalous southward energy transport arises from a slowdown of the upper cell of the oceanic meridional overturning circulation and a weakening of the horizontal ocean gyres, causing sea ice in the Northern Hemisphere to expand and the Arctic to cool. Comparison with a slab-ocean simulation confirms the importance of ocean dynamics in determining the climate system response to Antarctic orography. This paper concludes by briefly presenting a discussion of the relevance of these results to climates of the past and to future climate scenarios.

1. Introduction

Antarctica is among the largest plateaus on Earth, and its ice cover (and, consequently, surface orography) has fluctuated dramatically even while it has occupied its polar position. In this study, we investigate how the orography of the Antarctic Ice Sheet (AIS) influences the earth's climate system. We use a coupled atmosphere, ocean, land, and sea ice model (i.e., fully coupled) to study how local and remote responses to orography removal are facilitated through energy balance requirements and global teleconnections.

While the Antarctic continent assumed its polar position nearly 100 million years before present (mya), the initial glaciation of Antarctica occurred over the Eocene–Oligocene boundary [34 mya; see Lear et al. (2000) and Zachos et al. (2001)]. This glaciation was concurrent with the isolation of the continent as the Drake Passage opened and circumpolar ocean flow commenced (Kennett 1977), suggesting a strong association between ocean circulation and the AIS from the start. On the other hand, others have contested the role of Drake Passage opening in initiating Antarctic glaciation (Zhang et al. 2011; Goldner et al. 2014). A decrease in atmospheric CO_2 levels and changes in orbital parameters that favored cooler Southern Hemisphere (SH) summers are other factors that may have contributed to this initial glaciation (DeConto and Pollard 2003). Over the past 5 million years, paleoclimatological proxy evidence (Scherer 1991; Lisiecki and Raymo 2005) and modeling studies (Pollard and DeConto 2009) suggest that the West Antarctic Ice Sheet has been particularly sensitive to changes in orbital parameters and fluctuations in atmospheric greenhouse gas concentrations [see also the review by Robin (1988) and references therein].

In general, surface orography can affect the local angular momentum balance of the atmosphere, altering the winds at the surface and aloft, the jet and midlatitude storm track, and climate variability. Steering by orography affects the position of major atmospheric features, including arid zones and monsoonal circulations (Manabe and Terpstra 1974; Hahn and Manabe 1975; Manabe and Broccoli 1990). Following the pioneering research of Manabe and Terpstra (1974), many ensuing studies have further investigated climate responses to midlatitude orography, including that due to the Andes (Ehlers and Poulsen 2009; Sepulchre et al. 2009; Poulsen et al. 2010; Feng and Poulsen 2014), Himalayas (Ruddiman and Kutzbach 1989; Boos and Kuang 2010; Kitoh et al. 2010; Xu et al. 2010), and Rockies

Corresponding author address: Hansi Singh, Dept. of Atmospheric Sciences, University of Washington, Box 351640, Seattle, WA 98195.
E-mail: hansi@atmos.washington.edu

DOI: 10.1175/JCLI-D-15-0442.1

(Ruddiman and Kutzbach 1989; Seager et al. 2002; Takahashi and Battisti 2007). The climate impact of the orography from the Laurentide and Fennoscandian Ice Sheets at the Last Glacial Maximum has also been studied extensively, starting with Manabe and Broccoli (1985).

Many modeling studies have simulated past (and future) climates in which the orography of the AIS has been (or is projected to be) substantially lower than at present. Goldner et al. (2014) used a coupled GCM with an Oligocene–Eocene configuration of continents, sea level, and solar insolation to study the initial glaciation of Antarctica 34 mya. They found that a modest decline of CO_2 that, in turn, initiated the expansion of land ice over Antarctica (thereby raising both orography and albedo), was sufficient to invigorate the ocean circulation and cause the dramatic changes in ocean hydrography, surface winds, and deep water formation as seen in paleoproxy data. Opening of the Drake Passage or Tasman Gateway, on the other hand, did not produce such a similar rapid reorganization of the ocean circulation and hydrography. Knorr and Lohmann (2014) used GCM time-slice experiments to study the middle Miocene transition 13 mya, which was characterized by global cooling and expansion of the AIS to nearly its present-day volume. They found that on 100 000-yr time scales, the response of their model's winds, surface temperatures, sea ice, and ocean circulation due to AIS expansion alone was consistent with paleoproxy data. Only on million-year time scales and longer was atmospheric CO_2 drawdown necessary in their model to cause the global cooling seen in the paleoproxy data.

These and other paleoclimate modeling studies provide interesting insights into the impact of AIS orography on the Earth climate system, and suggest that AIS orography may affect the ocean circulation. Nevertheless, while these studies do isolate the effect of lowered orography on the climate system, they do so in climate states that are vastly different from that of the present day, particularly in terms of continental geography, ocean basin configurations, orbital parameters, and greenhouse gas concentrations.

On the other hand, a few studies have considered the impact of AIS orography on global climate in atmosphere-only GCMs (AGCMs) without such confounding factors. Several of these found enhanced poleward energy transport with lowered AIS orography (Mechoso 1981; Parish et al. 1994; Walsh et al. 2000; Ogura and Abe-Ouchi 2001), enhanced poleward momentum transport (Mechoso 1980, 1981; Parish et al. 1994; Simmonds and Law 1995; Walsh et al. 2000), decreased cyclogenesis over the Southern Ocean (Mechoso 1980, 1981; Simmonds and Law 1995; Walsh et al. 2000), and a weakening and poleward shift of the region of maximum baroclinicity (Mechoso 1980, 1981; Parish et al. 1994; Simmonds and Law 1995; Quintanar and Mechoso 1995; Walsh et al. 2000). While most of these studies used prescribed SSTs, Ogura and Abe-Ouchi (2001) showed that the local atmospheric circulation response to removing Antarctic orography tends to be similar but weaker when an AGCM is coupled to a mixed layer ocean compared with the same AGCM run with prescribed SSTs. Further, the significant surface wind response found in all of these experiments, given the sensitivity of the Southern Ocean circulation and Antarctic sea ice to surface wind forcing, motivates further study of this problem using models that can capture dynamical coupling with the ocean.

As far as we know, the work of Justino et al. (2014) is the only study that has isolated the climate impact of AIS orography in a fully coupled GCM in a climate state similar to that of the present day. However, the results of Justino et al. (2014) are surprising. Unlike many previous studies that have linked increased poleward energy transport with flattening of the AIS (e.g., Mechoso 1981; Parish et al. 1994; Walsh et al. 2000; Ogura and Abe-Ouchi 2001), Justino et al. (2014) found that the poleward energy transport in the SH decreased when the AIS was lowered by 25%. It is unclear whether this major discrepancy can be attributed to the use of a fully coupled GCM by Justino et al. (2014), or if this difference is due to the greater topography retained in Justino et al. (2014) compared to previous studies.

In this study, we isolate the climate impact of lowering AIS orography in both a fully coupled GCM and a companion model with a mixed-layer-only (slab) ocean. Our strategy allows us to investigate the important role of ocean dynamics on the climate response to lowering the AIS.

As expected, we find that lowering the AIS (while leaving the surface albedo unchanged) results in local surface warming of Antarctica. In addition, we find a range of remote effects on winds at the surface and aloft, equatorial precipitation, the ocean's meridional overturning and surface gyre circulations, and sea ice in both hemispheres. We find that the scope of these global changes can be understood in terms of energy balances maintained by oceanic and atmospheric energy transports.

2. Experimental setup

To explore the climate impact of lowering AIS orography, we performed a fully coupled simulation using the Community Climate System Model, version 4.0 (CCSM4; Gent et al. 2011). The atmosphere component has a finite-volume dynamical core, a horizontal resolution of 1.9° × 2.5°, and 26 vertical levels. The horizontal grid of the land component is the same as that of the atmosphere. The ocean and sea ice lie on a nominally

TABLE 1. Summary of preindustrial settings (solar insolation, greenhouse gas concentrations, and aerosol forcing) used in all simulations.

Constituent	Concentration or value	Notes
Total solar irradiance	1360.9 W m^{-2}	Mean of 1844 to 1856 irradiance
CO_2	284.7 ppm	
N_2O	275.7 ppb	
CH_4	791.6 ppb	
Aerosol forcing	−0.033 W m^{-2}	Equivalent aerosol forcing

1°-resolution displaced-pole grid, with the North Pole singularity centered within Greenland. The ocean eddy parameterization is a Gent and McWilliams (GM) form (Gent and McWilliams 1990), with the GM coefficient varying in space and time (Danabasoglu et al. 2012). The sea ice is fully thermodynamic and dynamic (Hunke and Lipscomb 2008).

As a baseline for comparison, we use a preindustrial control simulation with the CCSM4 run at the same resolution (hereafter referred to as C) in which ozone, carbon dioxide, and other greenhouse gases, volcanic constituents, and solar insolation are all held fixed at preindustrial levels (see Table 1). The experimental flat Antarctic run (hereafter referred to as FA) was branched from C at year 700 and had all parameters set as in C, but with the orography of Antarctica replaced by one in which the elevation is 10% of the original (present day) value (see Fig. 1 for the elevation anomaly). The surface albedo and orography standard deviation are unchanged. We ran FA for 230 yr to near equilibrium such that upper- and deep-ocean temperature trends in FA were statistically indistinguishable from those in C (referred to hereafter as quasi equilibrium). Results are presented as annual climatologies of the final 30 yr of the simulations (years 900–929 for C and 200–229 for FA). The net annual top-of-the-atmosphere (TOA) flux imbalance in the climatologies is 0.13 W m^{-2} for FA and 0.05 W m^{-2} for C. All quantities are annual means, unless otherwise noted. All zonal averages only include points that lie above the model surface; no extrapolation at pressure levels below the surface is performed. Transient covarying quantities are computed as

$$\overline{a'b'} = \overline{ab} - \overline{a}\,\overline{b}, \tag{1}$$

where $\overline{(\ )}$ is the monthly mean. Statistical significance of the difference in climatologically averaged quantities in FA and C is computed using a Student's t test with 29 degrees of freedom. The variance is estimated from a 300-yr time series of C.

We isolate the role of the ocean dynamics in the climate response to lowering the AIS by comparing results from fully coupled C and FA simulations to results from a pair of runs where we replace the ocean GCM with a slab ocean model (known hereafter as SOM). All other model components are otherwise identical. The control and flat Antarctic experiments with the SOM (known hereafter as CSOM and FASOM, respectively) differ from one another only in their AIS surface orography, with the same surface orography anomaly in FASOM as in FA. In both SOM runs, the ocean energy transport flux convergence field (often called q flux) was prescribed to be annually periodic but spatially heterogeneous from a monthly climatology derived from C (Bitz et al. 2012). Results are presented as climatologies of the final 30 yr of 60-yr runs, which can be considered to be at equilibrium.

We present the response to lowering AIS as the anomaly FA minus C in sections 3a–3e. The role of ocean dynamics is investigated by comparing FA minus C with FASOM minus CSOM in section 3f.

3. Results

a. Temperature response and energy balance

The local response to lowering AIS orography is a strong surface warming over most of East Antarctica and a mixed pattern of warming and cooling over West Antarctica. Remote surface cooling away from the AIS dominates

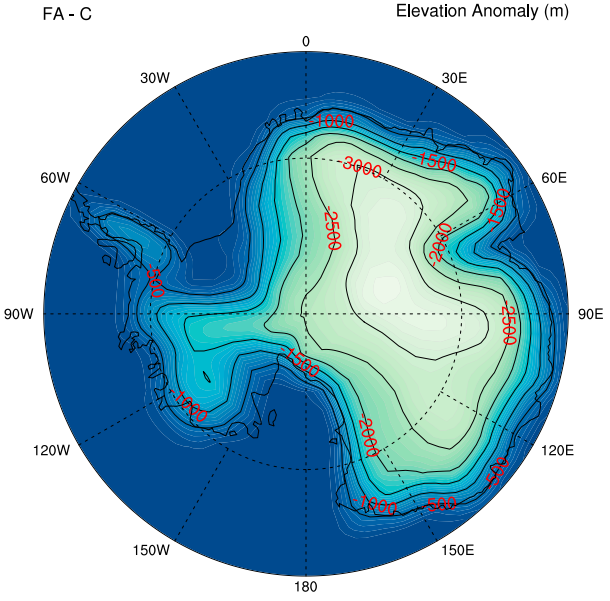

FIG. 1. Elevation anomaly (m) imposed over Antarctica in the FA and FASOM experiments, expressed as the difference FA C. Contours are drawn from 500 to 3000 m at intervals of 500 m.

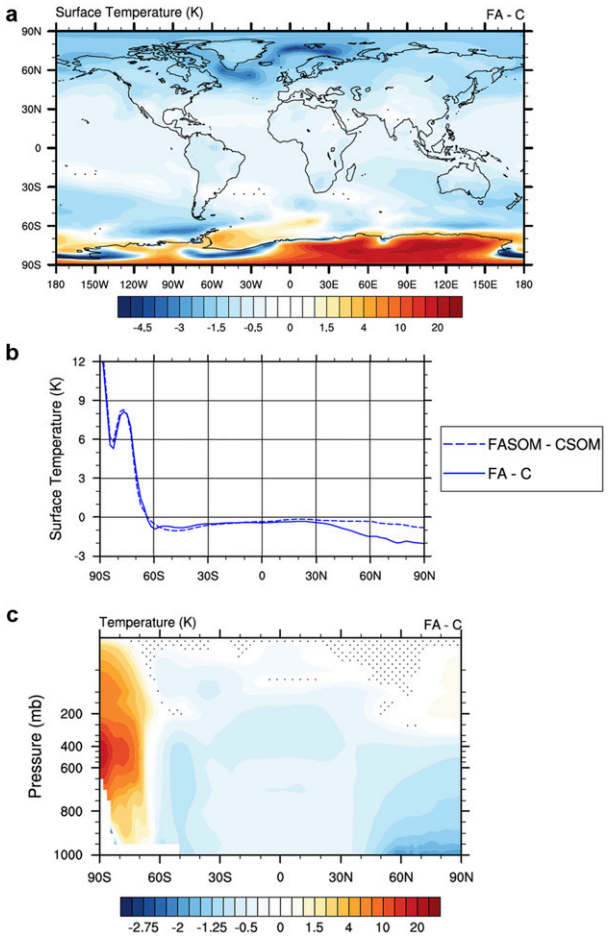

FIG. 2. Temperature response to lowering the AIS: (a) surface temperature in FA − C, (b) zonally averaged surface temperature in FA − C and FASOM − CSOM, and (c) zonally averaged atmospheric temperature in FA − C. Stippled areas in (a) and (c) indicate regions where the temperature anomaly is not statistically significant at $p < 0.05$. Note that positive and negative anomalies have been scaled asymmetrically to make negative anomalies more discernible.

the global mean surface temperature, however, which decreases by 0.3°C (see Figs. 2a and 2b). In the zonal mean, the atmosphere above the AIS warms from the troposphere to the stratosphere, while cooling over the Southern Ocean and in the Northern Hemisphere (NH) high latitudes remains confined to the surface and midtroposphere (Fig. 2c).

At the TOA, the outgoing longwave radiation (OLR) increases substantially over the AIS (Fig. 3a), driven by a temperature increase at the effective radiating level; this result is similar to that described by Ogura and Abe-Ouchi (2001). Although the AIS surface albedo is prescribed as that for a glaciated surface irrespective of elevation, the TOA absorbed shortwave (ASW) increases over the AIS because the warmer and deeper (by way of greatly increased surface pressure) atmosphere has much more precipitable water (not shown). Overall, the OLR increase wins out, and a larger amount of energy is lost to space over the AIS in FA. Partitioning the energetic fluxes between clear-sky and all-sky conditions shows that the TOA radiation anomalies over the AIS are predominantly clear sky. While an increase in low clouds plays a minor role in enhancing the OLR anomaly and diminishing the ASW anomaly, the TOA net radiative response due to clouds is modest (<10% of the total anomaly in the zonal mean). The enhanced energy loss to space over the continent implies that there must be anomalous southward energy transport (as shown in Fig. 4a).

The increased greenhouse effect of the warmer and deeper atmosphere increases the downwelling longwave (LW) radiation over the AIS (south of 60°S). The warming at the surface is unable to offset this effect and the net upward LW radiation decreases sharply (Fig. 3b). The surface ASW decreases, though by a smaller amount, as a result of increased atmospheric absorption. An increase in the (upward) sensible heat flux balances these surface radiative changes.

Enhanced cooling to space over the AIS in FA drives anomalous southward energy transport in both the atmosphere and ocean in the SH (Fig. 4a). This increase in southward energy transport near 60°S is a source of dynamical warming that augments the simple adiabatic warming due to lowering the AIS. The positive slope of the total energy transport anomaly from 60°S to 40°N (Fig. 4a) implies dynamical cooling throughout these latitudes.

The partitioning of the total energy transport anomaly between the ocean and atmosphere varies with latitude. In the SH high and middle latitudes, the atmosphere dominates, while the ocean transports most of the energy northward of 20°S. The direction of the atmospheric energy transport anomaly reverses around 20°N. Note that atmospheric and total energy transports are calculated implicitly, with the total energy transport computed from integrating (in latitude) the net TOA energy fluxes, and the atmospheric energy transport computed by integrating the difference between the TOA and surface energy fluxes. The oceanic energy transport is computed directly as a global integral of $v\theta$, where v is the meridional ocean velocity and θ is the potential temperature.

Southward atmospheric energy transport increases primarily because of increasing southward dry static energy (DSE) transport at all latitudes south of 20°N, with latent heat (LH) transport opposing the atmospheric energy transport anomaly at most latitudes (Fig. 4b). LH transport anomalies are northward from 65°S to 45°S, and from 20°S to 10°N; the former suggests both a northward shift in the midlatitude storm track and a decrease in poleward eddy moisture transport (due to decreased specific humidity with cooler temperatures north of 60°S,

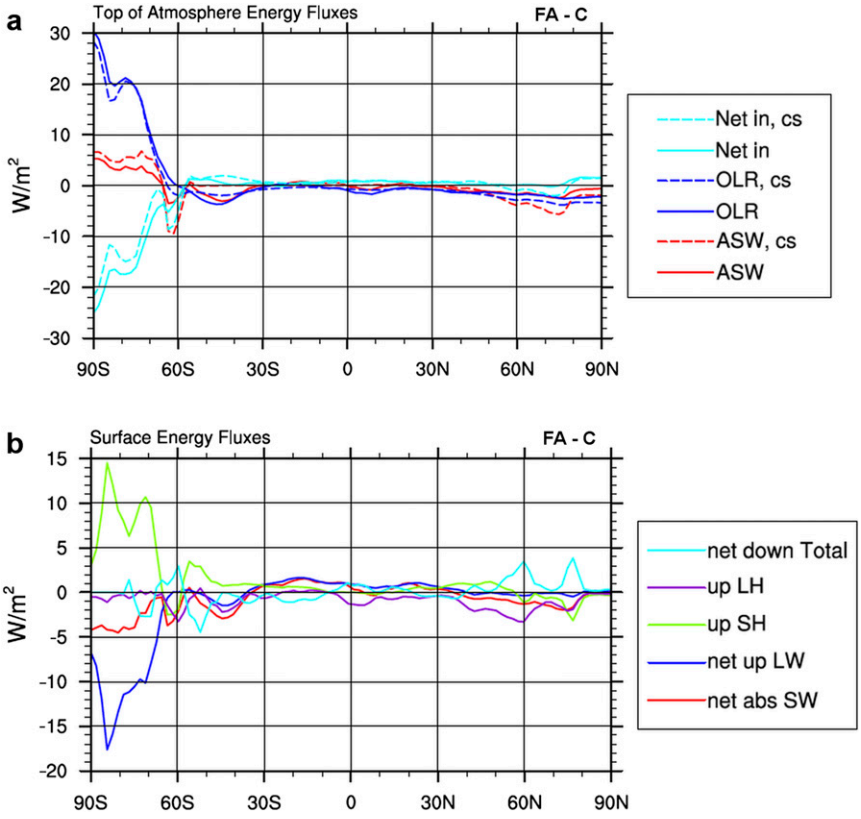

FIG. 3. Energetic response to lowering the AIS, expressed as the anomaly FA − C: (a) clear-sky (cs) and all-sky OLR, ASW, and net incoming radiation at the TOA and (b) net upward longwave radiation (net up LW), net absorbed shortwave radiation (net abs SW), upward sensible heat flux (up SH), upward latent heat flux (up LH), and net downward energy flux at the surface. Note that all fluxes are reckoned positive upward except the SW and net anomalies.

and a decreased meridional specific humidity gradient with strong warming over the AIS), while the latter suggests a northward shift in the rising branch of the Hadley circulation. Indeed, the response of the SH storm track and Hadley circulation is also evident in the global precipitation response (Fig. 10), which we address further in section 3e.

b. *Atmospheric circulation response*

Lowering the AIS alters the SH atmospheric circulation, which is evident in the zonal wind field (Fig. 5a). In FA, both the polar vortex and eddy-driven jet (at 65°S in the lower stratosphere and 55°S in the upper troposphere, respectively, in C) weaken on their poleward sides, the low-level easterly winds south of 65°S decelerate, and the surface and midtropospheric westerlies from 60° to 65°S accelerate slightly. These upper-level zonal wind responses are particularly strong in austral winter. At the surface, westerly winds decrease to the north and increase to the south of 60°S (Fig. 5b), decreasing the wind stress curl over the Southern Ocean.

Eddy driving of zonal wind changes is assessed using the transformed Eulerian mean framework, where the effect of eddies on the mean flow is analyzed using the spherical form of the quasigeostrophic Eliassen–Palm (EP) flux **F** (see Edmon et al. 1980; Holton 1992) given by

$$\mathbf{F} = a\cos\phi\left(-\overline{u'v'}, \frac{f_0 R}{N^2 H}\overline{v'T'}\right), \tag{2}$$

where $\overline{u'v'}$ is the meridional flux of zonal momentum by transient eddies, $\overline{v'T'}$ is the meridional flux of sensible heat by transient eddies, f_0 is the Coriolis parameter, R is the gas constant for dry air, N^2 is the Brunt–Väisälä frequency, and H is the atmospheric-scale height, a is the radius of the earth, and ϕ is the latitude. Figure 5c shows the effect of lowering the AIS on the EP flux vectors, and Fig. 5d shows the effect on the horizontal component of the EP flux (i.e., the meridional flux of zonal momentum by eddies). A strong increase in the EP flux convergence is evident at the poleward edge of the eddy-driven jet (near 60°S), consistent with its weakening (Fig. 5c). Figure 5d suggests that much of this increase in the EP

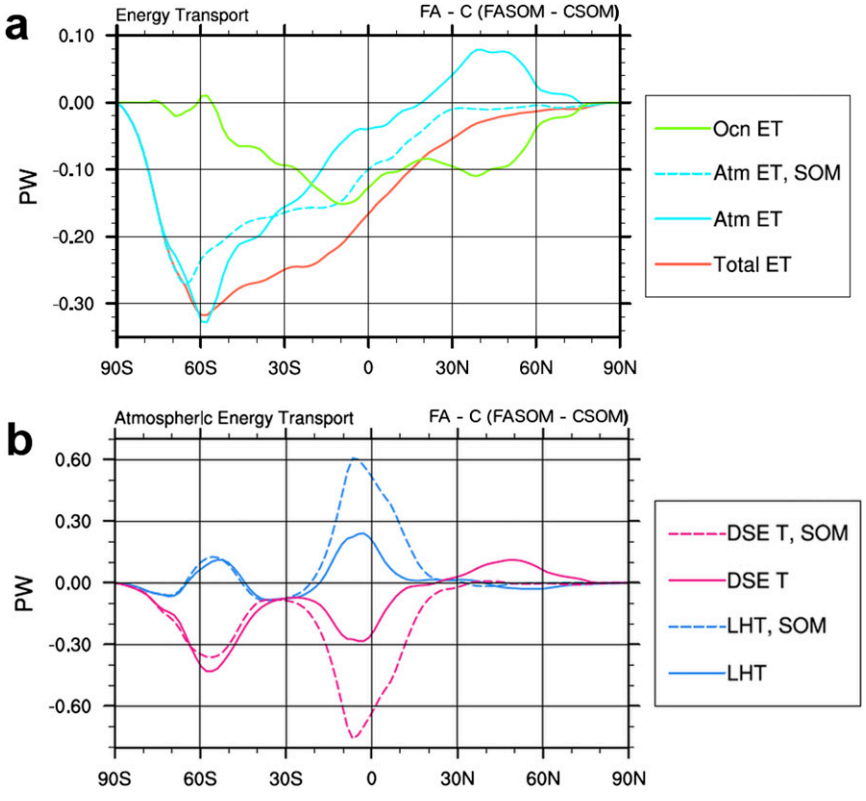

FIG. 4. Energy transport response to lowering the AIS (in PW), expressed as the anomaly FA − C or FASOM − CSOM: (a) total, atmospheric, and oceanic northward energy transport response and (b) breakdown of atmospheric northward energy transport response into dry static energy transport (DSE T) and latent heat transport (LHT).

flux convergence is due to a decrease in the meridional eddy momentum flux convergence. Similarly, the increase in the EP flux divergence south of 65°S is mostly due to a decrease in the meridional eddy momentum flux divergence. The EP flux divergence is negative here in C (not shown), which tends to decelerate the mean flow in this region; in FA, this convergence is reduced, resulting in a modest increase in the westerly winds here (Fig. 5a).

The absence of katabatic flow in FA helps weaken the SH eddy-driven jet. When the AIS is high, katabatic winds over Antarctica are downslope (gravity driven) flows that arise from strong pressure gradients created by surface radiative cooling; the easterly component arises from the need to balance surface drag with the Coriolis force (Parish and Waight 1987). When the AIS is lowered, katabatic flow ceases (Fig. 5a), and the accompanying westerly momentum transfer from the solid earth to the atmosphere above the AIS halts. As a result, northward momentum transport by atmospheric eddies near Antarctica is no longer required to balance the atmosphere's angular momentum budget (Fig. 5d), and the SH eddy-driven jet weakens on its poleward side.

The absence of katabatic flow in FA also explains the mixed pattern of warming and cooling over West Antarctica in FA (Fig. 6a). We define a temperature tendency due to katabatic winds as

$$\frac{dT}{dt} \equiv \frac{\mathbf{V} \cdot \nabla p}{\rho_0 R}, \tag{3}$$

where $\mathbf{V}$ is the surface velocity, ∇p is the climatological surface pressure gradient, ρ_0 is the reference air density, and R is the gas constant for dry air. This katabatic tendency results from adiabatic compression of air parcels transported by the surface wind in the direction of the surface pressure gradient. Equation (3) describes a cooling tendency in FA (compared to C) that is strongest near the AIS edge where the gradient of the orography is largest (Fig. 6b). The competing effect is warming with elevation loss at the dry-adiabatic lapse rate (Fig. 6c). Adiabatic warming dominates everywhere except over low-lying regions in West Antarctica, where the difference in elevation between FA and C is small but where katabatic flows in C are substantial.

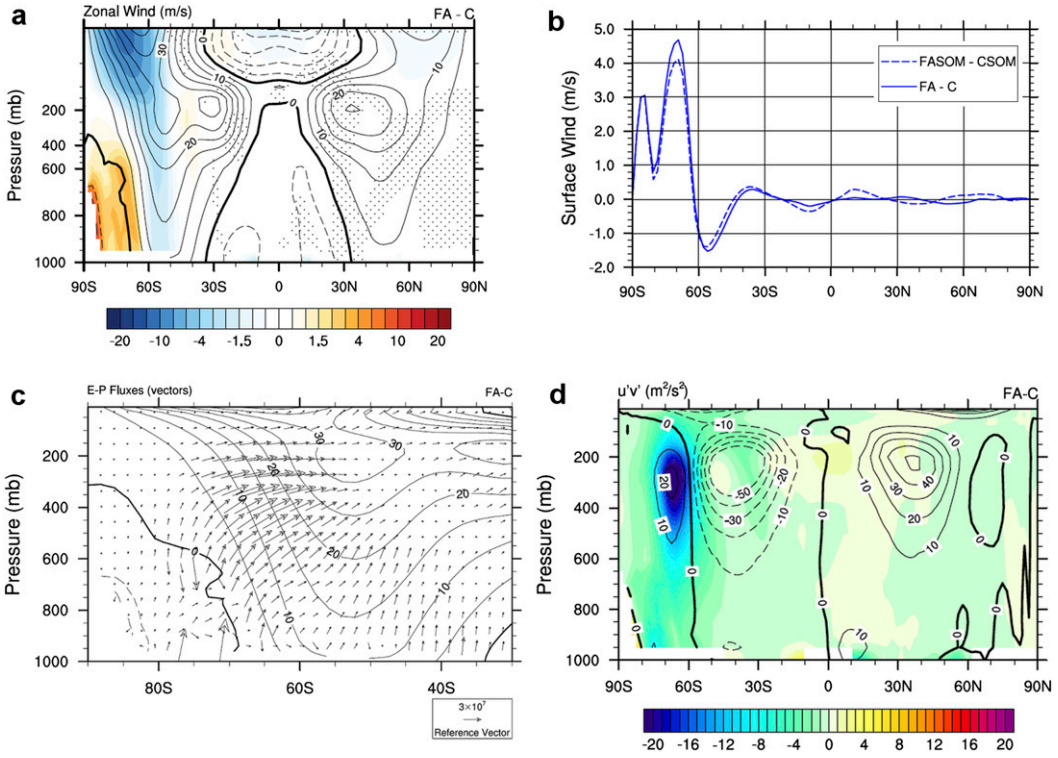

FIG. 5. Annually and zonally averaged momentum and zonal wind response to lowering the AIS: (a) zonal wind (in $m\,s^{-1}$); (b) surface winds in FA − C and FASOM − CSOM; (c) EP fluxes (in $m^2\,s^{-2}$, arrows) in FA − C, with zonal winds (contours) in C; and (d) eddy momentum flux $\overline{u'v'}$ (in $m^2\,s^{-2}$). In (a),(d), the contours depict the mean state C (with the zero contour thickened and negative contours dashed) and colors depict the anomaly FA − C. In (a), stippled areas indicate regions where the anomaly is not statistically significant at $p < 0.05$.

c. *Decomposing the atmospheric dynamical response*

To understand why southward atmospheric energy transport increases in the SH with lowering of the AIS, we evaluate changes in atmospheric transient eddy activity. In FA, eddy kinetic energy (EKE) increases in the troposphere south of 30°S (Fig. 7a). The largest increase in eddy activity is over the Antarctic continent (south of 65°S), a finding that agrees with the results of Mechoso (1981), Parish et al. (1994), Simmonds and Law (1995), and Walsh et al. (2000): while lowering the AIS decreases the rate of cyclogenesis over the Southern Ocean, it permits storms to form and intensify over the Antarctic continent itself and increases the average lifetime of storms at all latitudes (Mechoso 1981; Walsh et al. 2000). The latter effects dominate over the former, and poleward energy transport by atmospheric eddies increases, as seen in FA.

Enhanced cyclogenesis over the continent is made possible by enhanced baroclinic instability. Walsh et al. (2000) reformulated the baroclinic instability criterion of the two-layer quasigeostrophic model (see Holton 1992) from pressure levels to sigma levels in order to compare baroclinicity in experiments with varying AIS orography. On sigma levels, the criterion for baroclinicity can be written as

$$B \equiv \frac{2\lambda^2 U_T}{\beta} > 1, \tag{4}$$

where U_T is the vertical wind shear, β is the rate of change of the Coriolis parameter with latitude (with a correction for sigma coordinate conversion), and λ is the characteristic eddy wavelength as determined by the static stability:

$$\lambda^2 \sim \frac{\theta}{\partial\theta/\partial\sigma}. \tag{5}$$

The wind shear and the characteristic eddy wavelength are both evaluated at the $\sigma = 0.5$ vertical level. For further details on the quasigeostrophic two-layer model and derivation of the instability criterion on σ levels, see Holton (1992) and Walsh et al. (2000).

Figure 7b shows that B increases over the AIS, particularly over East Antarctica, and decreases over the Southern Ocean, particularly over the marginal ice zone

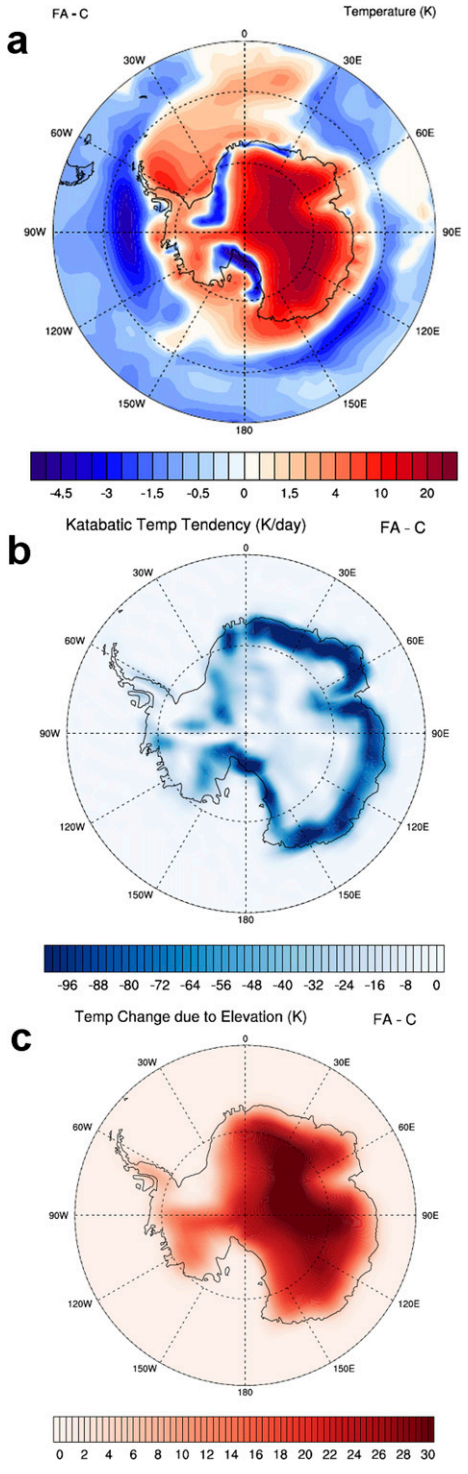

FIG. 6. Surface temperature response in the vicinity of the AIS in FA − C: (a) surface temperature (K), (b) temperature tendency due to katabatic winds (in K day^{-1}), and (c) temperature change (K) expected from the elevation change alone, assuming a dry-adiabatic lapse rate.

around the continent. Nevertheless, regions in which B decreases in FA are also regions in which B is already large, and such decreases in B are not substantial enough to suppress instability. Overall, a larger area satisfies the baroclinic instability criterion $B > 1$ in FA.

As expected from increased baroclinicity over much of the AIS, Fig. 7c shows that the southward sensible heat flux by atmospheric eddies $(\overline{v'T'})$ increases in FA. The increase is most pronounced on the southern flank of the climatological storm track, where $\overline{v'T'}$ doubles in FA, compared to C. Overall, the southward sensible heat flux by eddies increases at all latitudes south of 30°S. In Fig. 7c, we show the change in eddy heat transport on sigma coordinate levels ($\sigma = p/p_s$) in order to highlight how surface focused this anomaly is. The greater surface pressure in FA than in C permits eddies to transport more energy poleward (recall Fig. 4a), as there is more atmospheric mass through which baroclinic instability can act.

While EKE increases in the SH troposphere, EKE decreases in the stratosphere at the poleward edge of the polar vortex (Fig. 7a), suggesting that both decreased stratospheric wave driving and increased diabatic heating play a role in weakening the polar vortex (Haynes et al. 1991). Deceleration of the polar vortex in FA is consistent with a decreased pole-to-equator temperature gradient (recall Fig. 2c) since vertical wind shear must decrease by thermal wind balance.

d. *Ocean circulation and sea ice response*

Significant changes in surface winds in FA (Fig. 5b) suggest that AIS orography may be influential in shaping the ocean circulation and its energy transport. In fact, changes in surface wind stress account for changes in the wind-driven gyre circulation in FA that weaken northward energy transport by the ocean (Fig. 4a). Over the Atlantic, slowing surface westerlies (not evident in the zonal mean winds shown in Figs. 5a,b) cause the upper branch of the subtropical gyre to move southward, the Gulf Stream to weaken, and the subpolar gyre to weaken (Fig. 8a), resulting in an equatorward shift of the North Atlantic Drift and a decrease in ocean energy transport into the North Atlantic (Fig. 8c). Slowing and equatorward contraction of the surface westerlies is consistent with the significant NH cooling in FA (Chen et al. 2008).

The global oceanic meridional overturning circulation (MOC), whose streamfunction is shown in Fig. 8b, also transports less energy northward in FA (Fig. 8c). The upper cell of the MOC weakens over most latitudes and depths while the deep cell strengthens below 1500 m [see Marshall and Speer (2012) for a review of the upper and lower cells], consistent with less cross-equatorial energy transport by the ocean (and in agreement with Fig. 4).

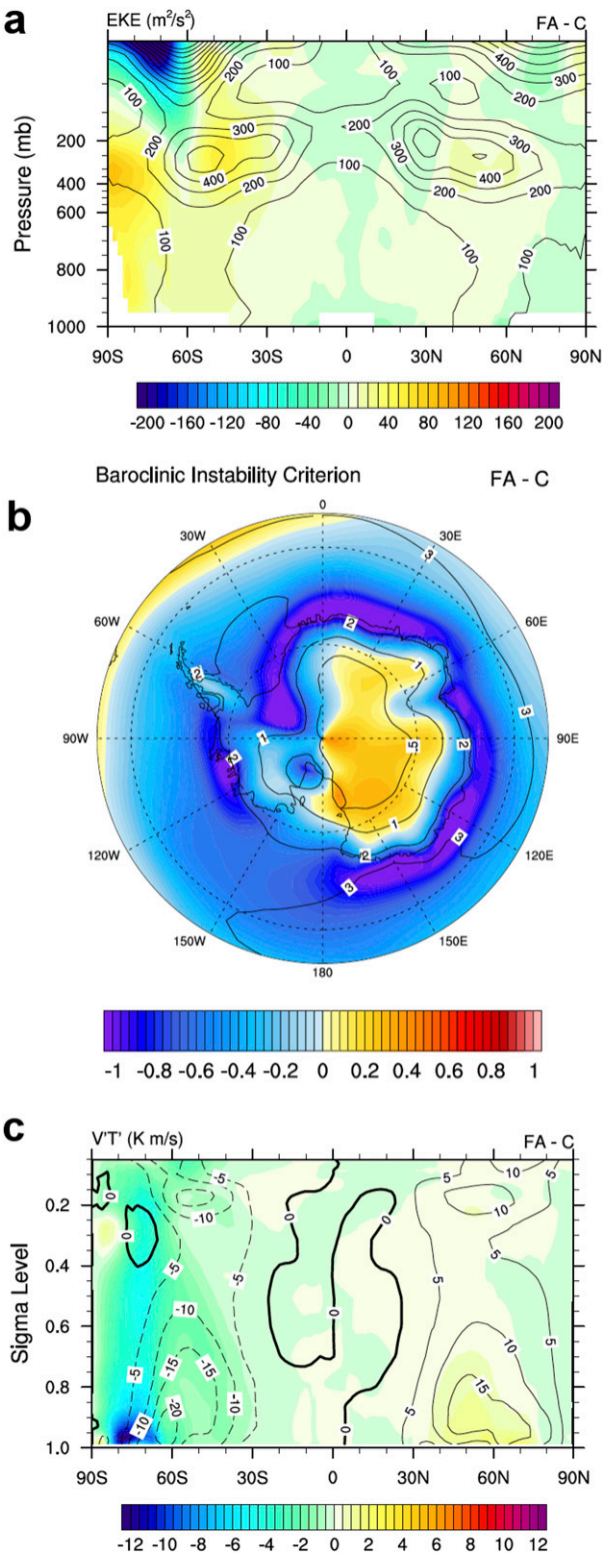

FIG. 7. Atmospheric eddy response to lowering the AIS: (a) annually averaged EKE (in $m^2 s^{-2}$), (b) baroclinic instability criterion B as described in Eq. (4), and (c) eddy sensible heat transport, $\overline{v'T'}$ (in K $m s^{-1}$), computed on sigma levels. In all panels, contours depict the mean state in C, and the anomaly FA–C is shown in colors.

As a consequence, the NH mid- and high latitudes cool, and Arctic sea ice, which depends sensitively on ocean energy transport (see Bitz et al. 2005), expands.

Sea ice, in fact, expands in both hemispheres (shown for the SH and NH in Figs. 9a and 9c, respectively), although the effect is larger and more ubiquitous in the NH than the SH. In the SH, the sea ice thins and expands nonuniformly about Antarctica, with the sole region of contraction in the Weddell sector. In the NH, the sea ice expands into the Greenland Sea, Bering Sea, Barents Sea, and south of Greenland. The decrease in ocean energy transport into the northern North Atlantic is dominated by weakening of the Atlantic meridional overturning circulation.

The surface westerly winds strengthen south of 60°S over the sea ice in the Southern Ocean (Fig. 5b). The resulting enhanced westerly momentum transfer to the ocean causes northward Ekman transport around the Antarctic margin; in such an ice-covered region, this momentum transfer also results in northward and eastward Ekman drift of sea ice [the turning angle of sea ice is approximately 45° relative to the direction of the wind, as described by Lepparanta (2011)]. As a consequence, Antarctic sea ice expands in most sectors (Fig. 9a) (Hall and Visbeck 2002). Although sea ice expands and surface buoyancy loss increases, the deep cell weakens (above 1500 m) because the wind stress curl over the Southern Ocean decreases (Fig. 5a), inhibiting Ekman suction of deep waters at the $\sigma = 27.6\,\mathrm{kg\,cm^{-3}}$ isopycnal (Marshall and Speer 2012).

e. *Precipitation response*

Figures 10a and 10b show that precipitation increases over the AIS while it decreases over the Southern Ocean, the latter a result of the midlatitude storm track shifting northward. The intertropical convergence zone (ITCZ) also shifts northward (Fig. 10a), which may be surprising given the decrease in temperature difference between the NH and SH [called the interhemispheric temperature anomaly in Friedman et al. (2013)]. However, the ITCZ shift is consistent with the need to balance TOA radiative energy loss over the AIS. Similar explanations that emphasize energetics driving ITCZ shifts have been offered by Chiang and Bitz (2005), Cheng et al. (2007), Kang et al. (2008), and Frierson and Hwang (2012). The northward ITCZ shift in our study is associated with an anomalous southward cross-equatorial flow in the upper troposphere, which facilitates anomalous southward cross-equatorial energy transport by the atmosphere.

The ITCZ shift also introduces a small, but significant, anomalous freshwater flux into the equatorial Atlantic of 0.01 Sv (1 Sv $\equiv 10^6\,m^3\,s^{-1}$; shown in Fig. 10b), slowing the upper cell of the MOC (shown in Fig. 8b) and facilitating anomalous southward energy transport by the ocean [a

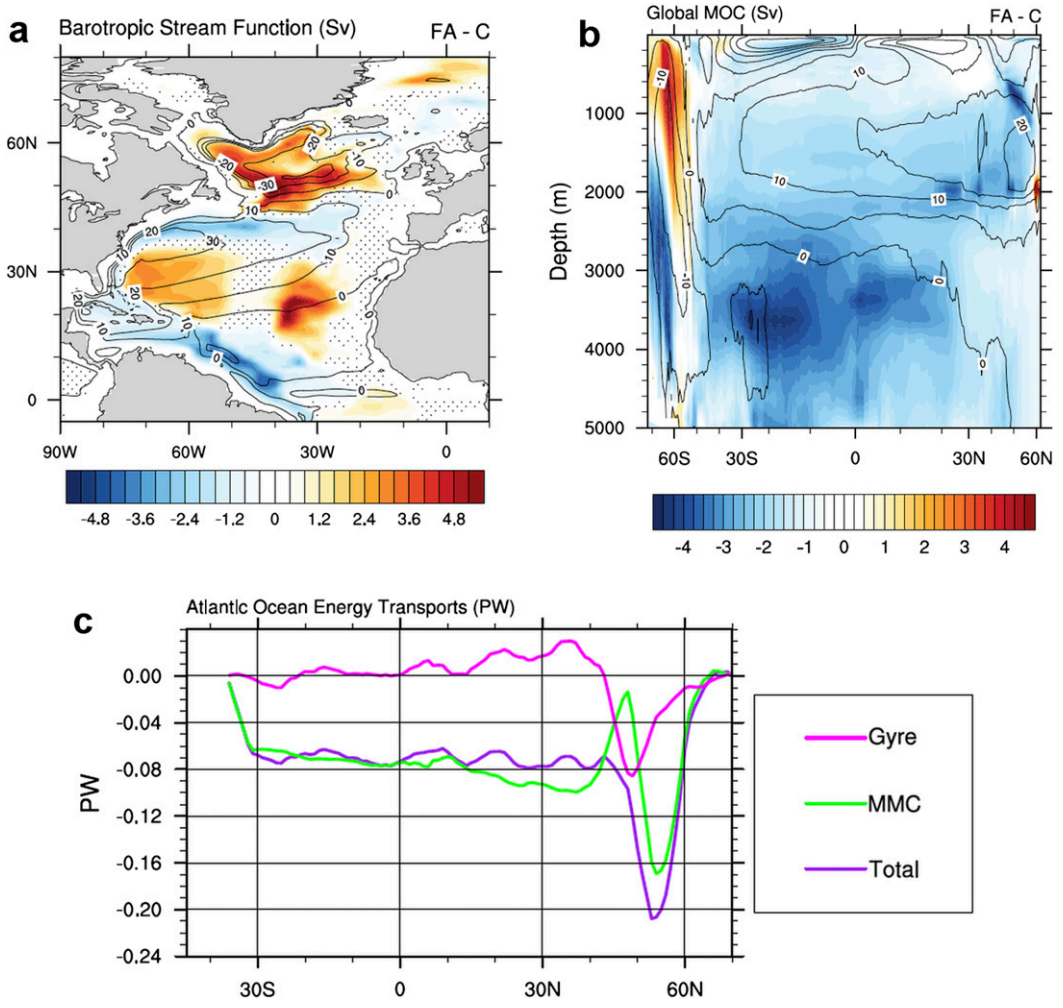

FIG. 8. Ocean dynamic response to lowering the AIS, with labeled contours depicting the mean state in C and colors depicting the anomaly FA − C: (a) annually averaged barotropic streamfunction [Sv (1 Sv $\equiv 10^6\,m^3\,s^{-1}$)] and (b) annually averaged global ocean meridional overturning streamfunction (Sv), shown as a function of depth; isopycnal flow has been removed by computing the streamfunction in potential density coordinates (σ) and converting to depth coordinates. The stippled areas in (a) indicate regions where the anomaly is not statistically significant at $p < 0.05$. In (b), the anomaly is statistically significant at $p < 0.05$ over more than 90% of the depth–latitude transect shown. (c) The total change in Atlantic basin energy transport, and the partitioning of this transport into gyre and mean meridional circulation (MMC) contributions.

mechanism described by Rahmstorf (1996)]. The shifting SH midlatitude storm track and its associated precipitation anomaly, on the other hand, are too far south and too weak to contribute significantly to slowing the MOC.

f. Isolating the role of ocean dynamics

To understand the role of ocean dynamics in the climate response to lowering the AIS, we compare the response in FASOM to that in FA. In FASOM, no adjustment of ocean energy transport is permitted, so only the atmospheric energy transport may respond to TOA energy perturbations. Nonetheless, the local climate response to lowering AIS orography is similar in FA and FASOM, with strong warming over the AIS and mild cooling over the Southern Ocean. The remote response, on the other hand, particularly that at the equator and the NH high latitudes, is significantly different in FA and FASOM, which we describe below.

Because the SOM cases were run to equilibrium, there can be no difference between the annual mean net surface heat flux in FASOM and CSOM. As a result, the anomalous atmospheric energy transport anomaly in FASOM is also the total energy transport anomaly. This transport anomaly resembles the total energy transport anomaly in FA, but is smaller in magnitude from 60°N to 60°S (Fig. 4a). As for FA, the total energy transport

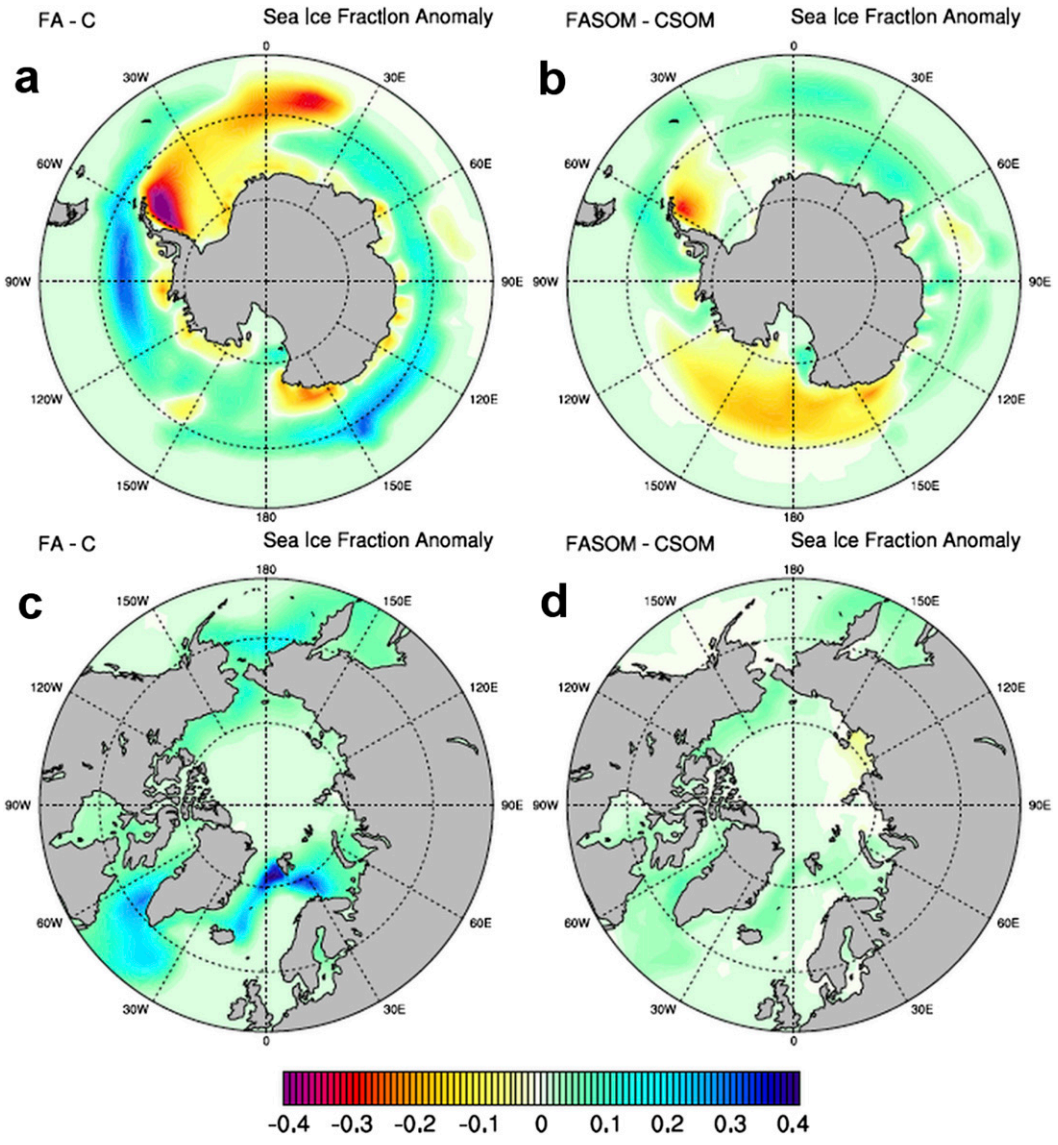

FIG. 9. Annually averaged sea ice response to lowering the AIS: (a) SH sea ice fraction in FA, expressed as FA − C; (b) SH sea ice fraction in FASOM, expressed as FASOM − CSOM; (c) NH sea ice fraction in FA, expressed as FA − C; and (d) NH sea ice fraction in FASOM, expressed as FASOM − CSOM.

response in FASOM offsets the TOA radiative cooling over the AIS, resulting in a warmer troposphere above Antarctica but a cooler one globally.

The southward energy transport anomaly in FASOM is significantly greater than the atmospheric component of the energy transport anomaly in FA from 30°N to 30°S, which corresponds to greater precipitation anomalies in the subtropics and tropics over all three ocean basins (see Figs. 10a–c, and Fig. 4b). The total cross-equatorial atmospheric energy transport anomaly, which is associated with the ITCZ shift and altered Hadley circulation, is about twice as large in FASOM as in FA. The magnitude of the tropical and subtropical atmospheric response must be larger in FASOM to satisfy the global energy balance in the absence of ocean energy transport anomalies. The larger ITCZ shift in FASOM relative to FA is also consistent with a larger northward shift in the equatorial SST maximum in FASOM (see Fig. 2b).

Long-range teleconnections between the lowered AIS and the NH high latitudes are also mediated by ocean dynamics. In the Arctic, surface temperature cooling in FA is greater than 2°C in the zonal average, while it is less than 1°C in FASOM (see Fig. 2b). The larger surface temperature response in FA is due to expanding sea ice (Fig. 9c); in FASOM, where the sea ice does not expand (Fig. 9d), the surface temperature response is muted

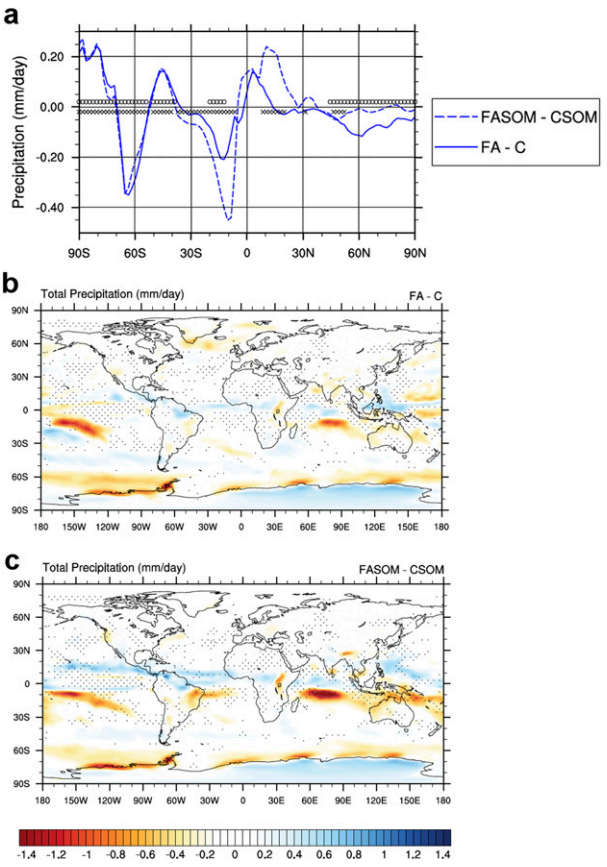

FIG. 10. Annually averaged precipitation response (mm day^{-1}) to lowering the AIS: (a) zonal mean, where circles (hatching) indicate latitudes where the precipitation anomaly in FA (FASOM) is statistically significant ($p < 0.05$); (b) FA − C, with stippled areas indicating regions where the anomaly is not statistically significant at $p < 0.05$; and (c) as in (b), but for FASOM − CSOM.

significantly. Sea ice expansion in FA is driven by decreased ocean energy transport into the northern high latitudes as a result of decreased transport by the horizontal gyre and (especially) overturning circulations (Fig. 8). In FASOM, where oceanic energy transport is held fixed, NH sea ice expansion and cooling do not occur as they do in FA.

4. Discussion

In undertaking this work, our objectives have been twofold: 1) to understand how the global climate responds to lowering the AIS and 2) to understand how incorporating ocean dynamics impacts this global climate response. By studying these climate impacts using a fully coupled GCM, we have been able to capture the global extent of how the climate system responds to lowering the AIS; by comparing the response in a fully coupled GCM to one in a GCM with a slab ocean, we have been able to pinpoint how coupling between the ocean and atmosphere shapes the way the global climate system responds.

We have shown that lowering the orography of the AIS has both local and global climatic consequences. While the surface and atmospheric column above the AIS warm, there is modest cooling over the Southern Ocean and globally. These temperature changes accompany a cessation of katabatic winds over the AIS, a weaker polar vortex, a slower jet, an equatorward shift of the midlatitude storm track, an expansion of the sea ice in both hemispheres, and a northward shift of the ITCZ. In the NH, northward energy transport by the oceanic MOC and wind-driven gyres decreases, and the Arctic cools. Globally, an increase in southward energy transport offsets higher TOA energy loss over the warmed AIS.

Figure 11 summarizes some of the energetic mechanisms at play in FA and FASOM, and illustrates the importance of atmosphere–ocean coupling in determining the cross-equatorial energy transport response to lowering the AIS. In both FA and FASOM, an increase in the OLR over the AIS prompts a net southward energy transport anomaly, which is of similar magnitude in the SH mid- and high latitudes. The slowing of the global MOC in FA causes anomalous southward cross-equatorial energy transport by the ocean, which permits less anomalous southward cross-equatorial energy transport by the atmosphere, leading to a significantly weaker ITCZ shift in the case with a dynamical ocean response.

In the FA case the ocean response provides some of the southward energy transport needed to offset the higher TOA energy loss over the AIS. Thus, the atmospheric energy transport in FA responds not only to the TOA radiative cooling over the AIS, but it also "compensates" for the ocean energy transport anomaly. Compensation is seen in a variety of GCMs (e.g., Frierson et al. 2007; Enderton and Marshall 2009), and is an expected result since the meridional distribution of TOA fluxes depends only weakly on the climate state (Stone 1978). However, the compensation is imperfect in our study since the total energy transport is different between the FA and FASOM cases; specifically, the total energy transport anomaly is more southward at all latitudes in FA compared to FASOM.

The deviations from perfect compensation can be understood by considering the atmospheric energy transport anomaly spreading the TOA and surface energy flux anomalies to other regions, a framework that has been used to explain energy transport changes with global warming in midlatitudes (Hwang and Frierson 2010) and high latitudes (Hwang et al. 2011). The weakened oceanic MOC in the FA simulation causes an anomalous surface heat flux into the atmosphere between 60° and 20°S, while there is an anomalous surface heat flux into the ocean

between 50° and 70°N (shown in Fig. 3b). The atmosphere responds by transporting much of the energy away, but radiates some to space locally. The latter leads to the lack of perfect compensation. Furthermore, some of the surface heat flux anomaly is due to vertical mixing and diffusion (in either the atmosphere or ocean) that is unrelated to horizontal energy transport, which also results in imperfect compensation.

Overall, our results agree with other AGCM and paleoclimate studies that have explored how the climate system responds to lowering the AIS. Ogura and Abe-Ouchi (2001) showed that flattening the AIS orography causes remote dynamical cooling; similarly, Knorr and Lohmann (2014) found remote dynamical warming when the AIS elevation was increased. Other AGCM studies have found enhanced poleward energy and momentum transports when the AIS is flattened (e.g., Mechoso 1981; Simmonds and Law 1995; Quintanar and Mechoso 1995; Walsh et al. 2000).

Enhanced southward energy transport when the AIS is lowered is a common result in AGCM studies with prescribed SSTs or slab oceans, including those of Mechoso (1981), Quintanar and Mechoso (1995), Simmonds and Law (1995), Walsh et al. (2000), and Ogura and Abe-Ouchi (2001). As shown by Ogura and Abe-Ouchi (2001), this anomalous energy transport arises to accommodate the greater TOA energy loss over the AIS. Indeed, the magnitude of the increase in southward energy transport associated with removing the AIS topography reported by Ogura and Abe-Ouchi (2001) is approximately 0.25 PW, which is nearly identical to that in our FASOM experiment. All of these studies concur that the enhanced southward energy transport is accomplished by baroclinic eddies.

We have also shown that the most remote response to lowering the AIS, the cooling of the Arctic and expansion of sea ice therein, is mediated by decreased ocean energy transport into the northern high latitudes. Neither the ocean cross-equatorial energetic response nor the cooling of the Arctic is possible in the results of Mechoso (1981), Parish et al. (1994), Simmonds and Law (1995), Quintanar and Mechoso (1995), and Ogura and Abe-Ouchi (2001) because these modeling studies do not incorporate ocean and sea ice dynamics. While the results of these earlier studies are not incorrect, they are incomplete because they do not take into account the ocean's ability to transport energy differently in response to changes in the surface energy balance brought about by the dynamic atmosphere response.

Why do SH eddies transport more energy poleward when the AIS is lowered, despite the reduction in the SH meridional temperature gradient and vertical wind shear? In our study, we find that the static stability ($d\theta/dz$) decreases over the AIS, and that this decrease has a greater impact on baroclinicity than does the decrease in wind shear. As a result, a greater area over the AIS satisfies the baroclinic instability criterion, permitting atmospheric eddies to grow and persist closer to the pole. These findings are similar to those of Walsh et al. (2000), who also found that baroclinically unstable regions expanded over the AIS when orography was removed. Furthermore, we note that SH atmospheric eddies are much more effective at transporting DSE poleward when the AIS is lowered since the surface pressure is much higher. Overall, eddies have a deeper atmospheric column through which to transport energy when the AIS is lowered; as a result, more energy is fluxed southward toward the AIS, offsetting the increase in OLR there and satisfying the required energy balance.

While our findings qualitatively agree with those of earlier AGCM and paleoclimate studies, they are at odds with those of Justino et al. (2014), the only other study to have considered the impact of AIS orography reduction in a fully coupled model without confounding factors. Justino et al. (2014) found that southward atmospheric energy transport decreased when the AIS was lowered by 25%. In their case, an increase in high clouds over the lower AIS decreased TOA OLR and decreased overall cooling over the AIS. None of the earlier AGCM studies found such an increase in high clouds to counteract enhanced radiative cooling over the warmer AIS. Furthermore, we find the cloud response in our experiments has only a minor impact on the TOA radiative flux anomaly. While we cannot rule out the increase in high clouds found by Justino et al. (2014), there is also no compelling reason to expect it should dominate the outcome.

Our findings suggest that lowering the AIS, in the absence of changes in greenhouse gases or other parameters, could result in modest global cooling, a counterintuitive result. The lowering of the AIS could act as a negative (stabilizing) feedback on anthropogenic climate change. Similarly, Knorr and Lohmann (2014) found that growth of the AIS acts as a negative feedback on its own expansion through wind and ocean circulation changes that tended to result in modest global warming. We find that the magnitude of the negative feedback associated with AIS collapse, however, is modest, and would likely be difficult to detect against the background of changes required to cause such a catastrophic loss of the AIS (as well as the concurrent meltwater flux associated with such a loss).

The purpose of this study is to isolate the effect of flattening AIS orography on climate from the effect of other major changes (such as decreased albedo over the AIS, increased freshwater fluxes into the Southern Ocean,

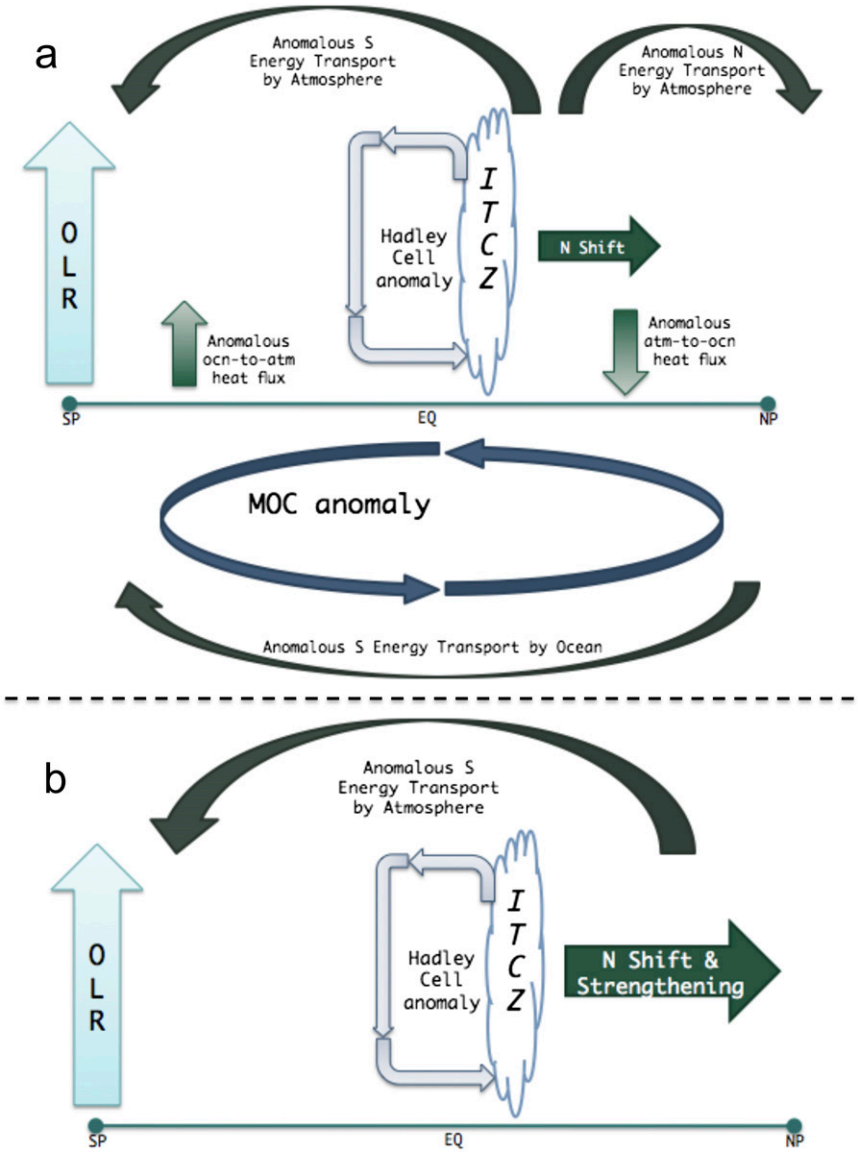

FIG. 11. Schematics summarizing the global energetic response to lowering the orography of Antarctica. (a) In the case of the fully coupled atmosphere and ocean (FA simulation), both the atmosphere and ocean energy transport processes respond to the enhanced OLR over Antarctica by increasing southward energy transport. Cross-equatorial energy transport is accomplished by a northward shift in the ITCZ and decreased transport by the upper cell of the oceanic MOC. (b) In the case of the (uncoupled) atmosphere and slab ocean (FASOM simulation), the atmosphere must accomplish all the southward cross-equatorial energy transport by shifting the ITCZ and the rising branch of the Hadley circulation northward more than it does in the coupled case.

and global sea level rise) that would doubtlessly accompany it. We do not aim to replicate climates of the past or future, and, as such, this is not a paleoclimate study; instead, we aim to isolate and study a single element of these climates, the impact of a negative orographic anomaly over the Antarctic continent, and, by doing so, to gain insight into the workings of the climate system.

Finally, it is important to note the limitations of this study. First, while our fully coupled experimental run may be considered to be near equilibrium, we point out that the deep ocean requires thousands of years to adjust fully to a perturbation, and it is possible that the equilibrium response to AIS lowering may differ significantly from that analyzed here. For example,

Danabasoglu and Gent (2009) show that for CO_2 doubling in a fully coupled model, the surface flux imbalance is still at 0.75 W m^{-2} at year 200, approximately one-fifth of the total flux imbalance introduced by the CO_2 forcing. While the TOA flux imbalance in FA is only 0.13 W m^{-2} at year 200, we cannot rule out further changes in the ocean circulation and energy partitioning that alter the atmospheric response. On the other hand, while we have considered the quasi-equilibrium response to lowering the AIS, the transient response is also of interest and is left for future work.

Furthermore, we have neither accounted for the different continental margins that would result if the AIS were to melt, nor accounted for the effects of meltwater on sea surface height and oceanic static stability, nor the decreased surface albedo over the AIS with melting. We speculate that decreased surface albedo over the AIS and an anomalously positive freshwater flux over the Southern Ocean would likely increase the importance of the dynamical mechanisms we have described in this study. A lower albedo over Antarctica would enhance warming at the surface and aloft locally, while increased freshwater input into the Southern Ocean would augment remote cooling by enhancing SH sea ice growth (via increased stability of the ocean mixed layer, which would decrease the entrainment and upwelling of warmer waters from below). Despite these caveats, the results presented herein are significant to the study of climate dynamics and the response of the climate system to high-latitude orography. Our study also elucidates the dynamics of past climates in which the AIS was lower or absent, and may be relevant to future climates with a lower AIS.

5. Conclusions

In this study, we have explored how AIS orography impacts the climate system. The high AIS orography of the present climate keeps Antarctica very cold and dry, and decreases TOA cooling; removing AIS orography, conversely, warms Antarctica at the surface and aloft, increases OLR over the continent, and enhances TOA cooling. As a result, southward energy transport toward Antarctica increases, with dynamical warming in the vicinity of the AIS but dynamical cooling over the rest of the globe.

Both atmospheric and oceanic processes contribute to increased southward energy transport. In the vicinity of the lowered AIS, the atmosphere is deep and permits baroclinic instability over a larger area, so eddies transport more DSE and zonal momentum southward. At the equator, more energy is transported southward cross equatorially by a northward shift in the rising branch of the Hadley cell and a weakened oceanic MOC. In the NH high latitudes, decreased northward energy transport by the ocean cools the Arctic and allows sea ice to expand into the North Atlantic and Pacific. Comparing the results from a fully coupled experiment to those from a slab-ocean experiment showed that atmosphere–ocean coupling is particularly important in determining the magnitude of the equatorial precipitation shift and the cooling of the Arctic.

In summary, we have detailed how the global climate system responds when AIS orography is reduced in the absence of confounding factors, and have identified the dynamic mechanisms involved in this response. We have studied this problem in a fully coupled GCM, and have isolated the role of ocean energy transport. Overall, the results of this study are relevant to understanding how the climate system adjusts to a perturbation and, in particular, how the atmosphere and ocean dynamically interact to produce a new quasi-equilibrium climate state.

Acknowledgments. We wish to acknowledge the U.S. DOE Computational Science Graduate Fellowship for funding HKAS, and NSF PLR-1341497 for funding CMB and DMWF. Thanks to Marc Michelson for computing support at the UW Department of Atmospheric Sciences. And thanks to Kat Huybers, Nathan Steiger, Ana Ordoñez, and Dennis Hartmann for helpful discussions and collaboration. We thank three anonymous reviewers for their helpful critique of our manuscript.

REFERENCES

Bitz, C., M. Holland, E. Hunke, and R. Moritz, 2005: Maintenance of the sea-ice edge. *J. Climate*, **18**, 2903–2921, doi:10.1175/JCLI3428.1.

——, K. Shell, P. Gent, D. Bailey, G. Danabasoglu, K. Armour, M. Holland, and J. Kiehl, 2012: Climate sensitivity of the Community Climate System Model, version 4. *J. Climate*, **25**, 3053–3070, doi:10.1175/JCLI-D-11-00290.1.

Boos, W., and Z. Kuang, 2010: Dominant control of the South Asian monsoon by orographic insulation versus plateau heating. *Nature*, **463**, 218–222, doi:10.1038/nature08707.

Chen, G., J. Lu, and D. Frierson, 2008: Phase speed spectra and the latitude of surface westerlies: Interannual variability and global warming trend. *J. Climate*, **21**, 5942–5959, doi:10.1175/2008JCLI2306.1.

Cheng, W., C. Bitz, and J. Chiang, 2007: Adjustment of the global climate to an abrupt slowdown of the Atlantic meridional overturning circulation. *Past and Future Changes in the Ocean's Meridional Overturning Circulation: Mechanisms and Impacts*, *Geophys. Monogr.*, Vol. 173, Amer. Geophys. Union, 295–313, doi:10.1029/173GM19.

Chiang, J., and C. Bitz, 2005: Influence of high latitude ice cover on the marine intertropical convergence zone. *Climate Dyn.*, **25**, 477–496, doi:10.1007/s00382-005-0040-5.

Danabasoglu, G., and P. Gent, 2009: Equilibrium climate sensitivity: Is it accurate to use a slab ocean model? *J. Climate*, **22**, 2494–2499, doi:10.1175/2008JCLI2596.1.

——, S. Bates, B. Briegleb, S. Jayne, M. Jochum, W. Large, S. Peacock, and S. Yeager, 2012: The CCSM4 ocean component. *J. Climate*, **25**, 1361–1389, doi:10.1175/JCLI-D-11-00091.1.

DeConto, R., and D. Pollard, 2003: Rapid Cenozoic glaciation of Antarctica induced by declining atmospheric CO_2. *Nature*, **421**, 245–249, doi:10.1038/nature01290.

Edmon, H., B. Hoskins, and M. McIntyre, 1980: Eliassen–Palm cross sections of the troposphere. *J. Atmos. Sci.*, **37**, 2600–2616, doi:10.1175/1520-0469(1980)037<2600:EPCSFT>2.0.CO;2.

Ehlers, T., and C. Poulsen, 2009: Influence of Andean uplift on climate and paleoaltimetry estimates. *Earth Planet. Sci. Lett.*, **281**, 238–248, doi:10.1016/j.epsl.2009.02.026.

Enderton, D., and J. Marshall, 2009: Explorations of atmosphere–ocean–ice climates on an aquaplanet and their meridional energy transports. *J. Atmos. Sci.*, **66**, 1593–1611, doi:10.1175/2008JAS2680.1.

Feng, R., and C. Poulsen, 2014: Andean elevation control on tropical Pacific climate and ENSO. *Paleoceanography*, **29**, 795–809, doi:10.1002/2014PA002640.

Friedman, A., Y.-T. Hwang, J. Chiang, and D. Frierson, 2013: Interhemispheric temperature asymmetry over the twentieth century and in future projections. *J. Climate*, **26**, 5419–5433, doi:10.1175/JCLI-D-12-00525.1.

Frierson, D., and Y.-T. Hwang, 2012: Extratropical influence on ITCZ shifts in slab ocean simulations of global warming. *J. Climate*, **25**, 720–733, doi:10.1175/JCLI-D-11-00116.1.

——, I. Held, and P. Zurita-Gotor, 2007: A gray-radiation aquaplanet moist GCM. Part II: Energy transports in altered climates. *J. Atmos. Sci.*, **64**, 1680–1693, doi:10.1175/JAS3913.1.

Gent, P., and J. McWilliams, 1990: Isopycnal mixing in ocean circulation models. *J. Phys. Oceanogr.*, **20**, 150–155, doi:10.1175/1520-0485(1990)020<0150:IMIOCM>2.0.CO;2.

——, and Coauthors, 2011: The Community Climate System Model version 4. *J. Climate*, **24**, 4973–4991, doi:10.1175/2011JCLI4083.1.

Goldner, A., N. Herold, and M. Huber, 2014: Antarctic glaciation caused ocean circulation changes at the Eocene–Oligocene transition. *Nature*, **511**, 574–577, doi:10.1038/nature13597.

Hahn, D., and S. Manabe, 1975: The role of mountains in the South Asian monsoon circulation. *J. Atmos. Sci.*, **32**, 1515–1541, doi:10.1175/1520-0469(1975)032<1515:TROMIT>2.0.CO;2.

Hall, A., and M. Visbeck, 2002: Synchronous variability in the Southern Hemisphere atmosphere, sea ice, and ocean resulting from the annular mode. *J. Climate*, **15**, 3043–3057, doi:10.1175/1520-0442(2002)015<3043:SVITSH>2.0.CO;2.

Haynes, P., C. Marks, M. McIntyre, T. Shepherd, and K. Shine, 1991: On the "downward control" of extratropical diabatic circulation by eddy-induced mean zonal forces. *J. Atmos. Sci.*, **48**, 651–678, doi:10.1175/1520-0469(1991)048<0651:OTCOED>2.0.CO;2.

Holton, J. R., 1992: *An Introduction to Dynamic Meteorology*. 3rd ed. International Geophysics Series, Vol. 48, Academic Press, 511 pp.

Hunke, E., and W. Lipscomb, 2008: CICE: The Los Alamos sea ice model. Documentation and software, version 4.0. Tech. Rep. LA-CC-06-012, Los Alamos National Laboratory, 115 pp.

Hwang, Y.-T., and D. Frierson, 2010: Increasing atmospheric poleward energy transport with global warming. *Geophys. Res. Lett.*, **37**, L24807, doi:10.1029/2010GL045440.

——, ——, and J. Kay, 2011: Coupling between Arctic feedbacks and changes in poleward energy transport. *Geophys. Res. Lett.*, **38**, L17704, doi:10.1029/2011GL048546.

Justino, F., J. Marengo, F. Kucharski, F. Stordal, J. Machado, and M. Rodrigues, 2014: Influence of Antarctic ice sheet lowering on the Southern Hemisphere climate: Modeling experiments mimicking the mid-Miocene. *Climate Dyn.*, **42**, 843–858, doi:10.1007/s00382-013-1689-9.

Kang, S., I. Held, D. Frierson, and M. Zhao, 2008: The response of the ITCZ to extratropical thermal forcing: Idealized slab-ocean experiments with a GCM. *J. Climate*, **21**, 3521–3532, doi:10.1175/2007JCLI2146.1.

Kennett, J., 1977: Cenezoic evolution of Antarctic glaciation, the circum-Antarctic Ocean, and their impact on global paleoceanography. *J. Geophys. Res.*, **82**, 3843–3860, doi:10.1029/JC082i027p03843.

Kitoh, A., T. Motoi, and O. Arakawa, 2010: Climate modelling study on mountain uplift and Asian monsoon evolution. *Monsoon Evolution and Tectonics—Climate Linkage in Asia*, P. D. Clift, R. Tada, and H. Zheng, Eds., Geological Society of London Special Publications, Vol. 342, 293–301, doi:10.1144/SP342.17.

Knorr, G., and G. Lohmann, 2014: Climate warming during Antarctic ice sheet expansion at the middle Miocene transition. *Nat. Geosci.*, **7**, 376–381, doi:10.1038/ngeo2119.

Lear, C., H. Elderfield, and P. Wilson, 2000: Cenozoic deep-sea temperatures and global ice volumes from Mg/Ca in benthic foraminiferal calcite. *Science*, **287**, 269–272, doi:10.1126/science.287.5451.269.

Lepparanta, M., 2011: *The Drift of Sea Ice*. 2nd ed. Springer-Praxis Books in Geophysical Sciences, Springer-Verlag, 347 pp.

Lisiecki, L. E., and M. E. A. Raymo, 2005: A Pliocene-Pleistocene stack of 57 globally distributed benthic $\delta_{18}O$ records. *Paleoceanography*, **20**, PA1003, doi:10.1029/2004PA001071.

Manabe, S., and T. Terpstra, 1974: The effects of mountains on the general circulation of the atmosphere as identified by numerical experiments. *J. Atmos. Sci.*, **31**, 3–42, doi:10.1175/1520-0469(1974)031<0003:TEOMOT>2.0.CO;2.

——, and A. Broccoli, 1990: Mountains and arid climates of the middle latitudes. *Science*, **247**, 192–195, doi:10.1126/science.247.4939.192.

——, and ——, 1985: The influence of continental ice sheets on the climate of an ice age. *J. Geophys. Res.*, **90**, 2167–2190, doi:10.1029/JD090iD01p02167.

Marshall, J., and K. Speer, 2012: Closure of the meridional overturning circulation through Southern Ocean upwelling. *Nat. Geosci.*, **5**, 171–180, doi:10.1038/ngeo1391.

Mechoso, C., 1980: The atmospheric circulation around Antarctica: Linear stability and finite-amplitude interactions with migrating cyclones. *J. Atmos. Sci.*, **37**, 2209–2233, doi:10.1175/1520-0469(1980)037<2209:TACAAL>2.0.CO;2.

——, 1981: Topographic influences on the general circulation of the Southern Hemisphere: A numerical experiment. *Mon. Wea. Rev.*, **109**, 2131–2139, doi:10.1175/1520-0493(1981)109<2131:TIOTGC>2.0.CO;2.

Ogura, T., and A. Abe-Ouchi, 2001: Influence of the Antarctic ice sheet on southern high latitude climate during the Cenozoic: Albedo vs topography effect. *Geophys. Res. Lett.*, **28**, 587–590, doi:10.1029/2000GL011366.

Parish, T., and K. I. Waight, 1987: The forcing of Antarctic katabatic winds. *Mon. Wea. Rev.*, **115**, 2214–2226, doi:10.1175/1520-0493(1987)115<2214:TFOAKW>2.0.CO;2.

——, D. Bromwich, and R.-Y. Tzeng, 1994: On the role of the Antarctic continent in forcing large-scale circulations in the high southern latitudes. *J. Atmos. Sci.*, **51**, 3566–3579, doi:10.1175/1520-0469(1994)051<3566:OTROTA>2.0.CO;2.

Pollard, D., and R. DeConto, 2009: Modelling West Antarctic ice sheet growth and collapse through the past five million years. *Nature*, **458**, 329–332, doi:10.1038/nature07809.

Poulsen, C., T. Ehlers, and N. Insel, 2010: Onset of convective rainfall during gradual late Miocene rise of the central Andes. *Science*, **328**, 490–493, doi:10.1126/science.1185078.

Quintanar, A., and C. Mechoso, 1995: Quasi-stationary waves in the Southern Hemisphere. Part II: Generation mechanisms. *J. Climate*, **8**, 2673–2690, doi:10.1175/1520-0442(1995)008<2673:QSWITS>2.0.CO;2.

Rahmstorf, S., 1996: On the freshwater forcing and transport of the Atlantic thermohaline circulation. *Climate Dyn.*, **12**, 799–811, doi:10.1007/s003820050144.

Robin, G., 1988: The Antarctic ice sheet, its history and response to sea level and climatic changes over the past 100 million years. *Palaeogeogr. Palaeoclimatol. Palaeoecol.*, **67**, 31–50, doi:10.1016/0031-0182(88)90121-6.

Ruddiman, W., and J. Kutzbach, 1989: Forcing of late Cenozoic Northern Hemisphere climate by plateau uplift in southern Asia and the American west. *J. Geophys. Res.*, **94**, 18 409–18 418, doi:10.1029/JD094iD15p18409.

Scherer, R. P., 1991: Quaternary and tertiary microfossils from beneath Ice Stream B: Evidence for a dynamic West Antarctic Ice Sheet history. *Global Planet. Change*, **90**, 395–412, doi:10.1016/0921-8181(91)90005-H.

Seager, R., D. Battisti, J. Yin, N. Gordon, N. Naik, A. Clement, and M. Cane, 2002: Is the Gulf Stream responsible for Europe's mild winters? *Quart. J. Roy. Meteor. Soc.*, **128**, 2563–2586, doi:10.1256/qj.01.128.

Sepulchre, P., L. Sloan, M. Snyder, and J. Fiechter, 2009: Impacts of Andean uplift on the Humboldt current system: A climate model sensitivity study. *Paleoceanography*, **24**, PA4215, doi:10.1029/2008PA001668.

Simmonds, I., and R. Law, 1995: Associations between Antarctic katabatic flow and the upper level winter vortex. *Int. J. Climatol.*, **15**, 403–421, doi:10.1002/joc.3370150405.

Stone, P., 1978: Constraints on dynamical transports of energy on a spherical planet. *Dyn. Atmos. Oceans*, **2**, 123–139, doi:10.1016/0377-0265(78)90006-4.

Takahashi, K., and D. Battisti, 2007: Processes controlling the mean tropical Pacific precipitation pattern. Part I: The Andes and the eastern Pacific ITCZ. *J. Climate*, **20**, 5696–5706, doi:10.1175/2007JCLI1656.1.

Walsh, K., I. Simmonds, and M. Collier, 2000: Sigma-coordinate calculation of topographically forced baroclinicity around Antarctica. *Dyn. Atmos. Oceans*, **33**, 1–29, doi:10.1016/S0377-0265(00)00054-3.

Xu, Z., Y. Qian, and C. Fu, 2010: The role of land–sea distribution and orography in the Asian monsoon. Part II: Orography. *Adv. Atmos. Sci.*, **27**, 528–542, doi:10.1007/s00376-009-9045-z.

Zachos, J., M. Pagani, L. Sloan, E. Thomas, and K. Billups, 2001: Trends, rhythms, and aberrations in global climate 65 ma to present. *Science*, **292**, 686–693, doi:10.1126/science.1059412.

Zhang, Z., K. Nisancioglu, F. Flatoy, M. Bentsen, I. Bethke, and H. Wang, 2011: Tropical seaways played a more important role than high latitude seaways in Cenozoic cooling. *Climate Past*, **7**, 801–813, doi:10.5194/cp-7-801-2011.